Release mechanism of octadecyl rhodamine B chloride from Au nanorods by ultrafast laser pulses

Citation: Alper, Joshua, Monica Crespo, and Kimberly Hamad-Schifferli. "Release Mechanism of Octadecyl Rhodamine B Chloride from Au Nanorods by Ultrafast Laser Pulses." The Journal of Physical Chemistry C 113.15 (2009): 5967-5973.

As Published: http://dx.doi.org/10.1021/jp809646e

Publisher: American Chemical Society

Persistent URL: http://hdl.handle.net/1721.1/49842

Version: Author's final manuscript: final author's manuscript post peer review, without publisher's formatting or copy editing

Release mechanism of octadecyl rhodamine B chloride from Au nanorods by ultrafast laser pulses

Joshua Alper[*], *Monica Crespo*[**], *Kimberly Hamad-Schifferli*[*,**,±]

[*] Department of Mechanical Engineering, Massachusetts Institute of Technology, 77 Massachusetts Avenue, Cambridge, MA 02139; [**] Department of Biological Engineering, Massachusetts Institute of Technology, 77 Massachusetts Avenue, Cambridge, MA 02139

schiffer@MIT.EDU

RECEIVED DATE

CORRESPONDING AUTHOR FOOTNOTE [±] To whom correspondence should be addressed. Tel: (617) 452-2385. Fax: (617) 258-0204. E-mail: schiffer@mit.edu.

ABSTRACT We investigated the release of octadecyl rhodamine B chloride (R_{18}) loaded onto cetyltrimethylammonium bromide (CTAB) coated gold nanorods (NR) by pulsed ultrafast laser excitation. R_{18} intercalates into the hydrophobic CTAB bilayer on the NR surface and can exchange on and off the NR with free CTAB micelles in solution. We find that laser excitation accelerates the rate of both R_{18} release from the NR and R_{18} binding to the NR with increasing fluence. However, at laser fluences > 220 $\mu J/cm^2$ thermal degradation of the R_{18} dominates. We also find that the concentration of CTAB, particularly around the critical micelle concentration, strongly influences the release and binding rates.

KEYWORDS. CTAB, exchange, micelle, delivery, surfactant ligand, surface chemistry

INTRODUCTION

Due to their unique optical properties, Au nanorods (NRs) are attractive for applications such as delivery,[1-5] surface enhanced Raman spectroscopy (SERS) substrates,[6,7] and tumor ablation.[8,9] Because the synthesis conditions tune the NR aspect ratio[10] and subsequently the wavelength of the longitudinal surface plasmon resonance (SPR),[11-13] NRs can be synthesized such that they absorb in the near infrared where water and tissue do not absorb light strongly.[14] Because the SPR is specific to the NRs, ps- and fs-pulsed laser excitation at the SPR specifically heats Au NRs and not the surroundings.[11,15,16] Consequently, NRs have been used for applications such as photothermal cancer therapy,[17] triggered delivery,[1-5] and targeted destruction of microorganisms.[18,19]

NR-mediated delivery is achieved by exciting the NR at the longitudinal SPR with ultrafast laser excitation. This specifically heats the NR, resulting in release of a payload that is either conjugated or adsorbed to the NR while leaving the surroundings unaffected.[1-5] Because biomolecules are sensitive to heat and prone to denaturation, particularly on nanoparticle surfaces,[20] the heat from NR ablation or melting may permanently damage the released species, substantially reducing delivery yield. Temperature increases of the NR upon absorption of ultrafast pulsed laser irradiation in the current state of the art release studies have been estimated to be ~100-1000 °C,[21-23] either limiting the payload to molecules robust enough to withstand these conditions or accepting a low delivery yield. Therefore, determining laser fluence limits for release while minimizing thermal degradation is desirable. In addition, the surface chemistry of the NR can affect release.

Cetyltrimethylammonium bromide (CTAB), the ligand that is required for NR synthesis,[24] is amphiphilic and forms a bilayer on the NR. CTAB comes on and off the NR surface, so the CTAB concentration most likely plays a role in release. Furthermore, the CTAB bilayer is known to affect the local thermal confinement of the NR upon laser excitation,[15,25] which could also influence release. Therefore, the CTAB layer's effect on release also needs to be determined.

Here, we demonstrate that the release of a small molecule from NRs by ultrafast laser excitation,

though complex, can be controlled through an understanding of the physical and practical limits on the critical release parameters. We discuss the mechanism, thermodynamics and kinetics of release. This document reports the release of octadecyl rhodamine B chloride (R_{18}) from Au NRs using ultrafast-pulsed laser excitation (Scheme 1). We quantify the R_{18} release rate as a function of laser fluence and CTAB concentration, and determine ranges of laser fluence that limit thermal degradation. Additionally, we describe how the release mechanism involves exchange of the R_{18} between the CTAB layer on the NR surface and free CTAB micelles.

MATERIALS AND METHODS

NR synthesis

Au NRs were synthesized in 50 mL batches using the non-seeding method.[26] 46 mL of 162 mM hexadecyltrimethylammonium bromide (CTAB) were added to 1.125 mL of 100 mM NaCl. 900 μL of 50 mM Au (III) chloride trihydrate ($HAuCl_4 \cdot 3H_2O$) and 675 μL of 10 mM silver nitrate ($AgNO_3$) were added, which turned the solution yellow-brown. After light agitation, 900 μL of 100 mM L-ascorbic acid (AA) were added, which turned the solution clear after ~30 s of agitation by inversion. 32 μL of 3.125 mM sodium borohydride ($NaBH_4$) were added, and the solution was agitated by inversion for ~30 s. The solution was left at room temperature for >3 h while it turned deep purple/brown. All chemicals used were obtained from Sigma-Aldrich, Inc. and used as supplied.

NRs were washed and concentrated by centrifugation for a time and speed dependent on the size of the sample, i.e. 15 min and 10,000 relative centrifugal force for a 1.5 mL solution. After centrifugation, the supernatant was removed and replaced with 1 mM CTAB. NRs were washed 3× to remove excess reagents. The NR solution was stored at 100 nM in 1 mM CTAB.

NR characterization

NR samples were prepared for transmission electron microscopy (TEM, JEOL 200CX) by drying ~15 μL of 100 nM Au NR solution on a copper grid with a carbon film (Ted Pella). >1400 NRs from five

images were sized with ImageJ version 1.37.[27] Synthesis yield is calculated by dividing the number of NRs by the total number of nanoparticles (rods and spheres). Au nanoparticles are considered spheres if their aspect ratio (AR = length/diameter) is <1.75. Optical absorption (Cary 50 UV/Vis Spectrophotometer) samples were ~0.5 nM NR solutions in 10 mM CTAB. NR concentration was calculated using an extinction coefficient for the longitudinal SPR of 1.9 x10^9 M^{-1} cm^{-1}.[28]

R_{18} loading of NRs

The fluorescent dye octadecyl rhodamine B chloride (R_{18}, Sigma-Aldrich – Fluka) was bound to the NRs by incubating 10 μL of 5 μM R_{18} in dimethyl sulfoxide with 1 mL of a 10 nM NR, 1 mM CTAB solution overnight. Loading occurs because the hydrophobic octadecyl group on the R_{18} packs in the CTAB layer on the surface of the NR.[29-31] The R_{18} loaded NRs were washed 2× by centrifugation to remove ~99% of the R_{18} not bound to NRs. Fluorescence intensity of the supernatant was used to estimate the coverage of R_{18} on NRs. The final stock solution consisted of 10 nM R_{18} loaded NRs in 0.1 – 1 mM CTAB.

Laser irradiation

Laser induced release: 13 μL of 10 nM R_{18} loaded NR stock were added to 104 μL of water. 13 μL of 100 mM CTAB was added to raise the CTAB concentration to 10 mM. A 65 μL aliquot of the sample was set aside at room temperature. The remaining 65 μL aliquot was placed in a 3 mm × 3 mm cuvette at the center of a 10 mm diameter laser spot. It was exposed to 60 – 1200 s of pulsed laser irradiation. Immediately after exposure, both aliquots were centrifuged to separate the NRs from the released R_{18}. The supernatant and precipitate from both aliquots were saved for analysis.

To generate the ultrafast pulsed laser irradiation, the 82 MHz output from a Ti:sapphire oscillator (Tsunami, Spectra-Physics) was amplified by a Ti:sapphire regenerative amplifier (Spitfire, Spectra-Physics) to produce 100 fs full width at half max, λ = 792 nm (Figure 1c) pulses at 1 kHz. The oscillator was pumped with a continuous wave 532 nm (Millennia, Spectra-Physics) laser and the amplifier was pumped with 1 kHz, 527 nm ns pulses (Empower, Spectra-Physics). The laser power was varied from

20 to 100 mW, which resulted in the fluence varying from 110 to 550 μJ/cm^2.

Laser accelerated loading: The procedure was identical to laser induced release, except that the sample consisted of 1.3 μL of 100 nM NRs added to 130 μL of a 150 nM R_{18} and 1 mM CTAB solution. All further processing of the sample was identical to the laser induced release procedure.

Water bath heating

Water bath induced release: The procedure was identical to the laser induced release procedure, except that one aliquot was heated in a water bath instead of being exposed to laser irradiation.

Water bath accelerated loading: The procedure was identical to water bath induced release except that the sample consisted of a 1.3 μL aliquot 100 nM Au NR stock added to 130 μL of a 150 nM R_{18} 1 mM CTAB solution.

Fluorescence spectroscopy

Fluorescence spectroscopy (HORIBA Jobin Yvon FluoroMax 3) of the supernatant was used to quantify the R_{18} released per NR for each sample. Fluorescence spectra of the sample supernatants diluted in 10 mM CTAB to 130 μL were taken, after NR separation, at $\lambda_{excitation}$ = 559 nm with slit sizes of 2 nm about the excitation and emission wavelengths in a 3 mm × 3 mm cuvette. The fluorescence intensity of the unexposed, room-temperature aliquot was subtracted from the exposed aliquot yielding the change in supernatant intensity, and subsequently the change in concentration of R_{18} associated with CTAB micelles. Because the room temperature release rate was slow compared to the laser irradiated and water bath release rates, we assume that the room temperature release rate is negligible over the course of our experiments. Thus, the change in the number of R_{18} molecules associated with CTAB micelles per NR equals the number of R_{18} molecules released per NR. The rate of R_{18} release is found by calculating the slope of the R_{18} released vs time data. The rate of release, in (R_{18}/(NR·s)), can be converted to release per pulse by dividing by the repetition rate of the laser (1 kHz). This also represents the probability of releasing an R_{18} molecule with a single pulse, or the average number of R_{18} molecules released per NR per pulse.

Solvent heating experiments

A K-type thermocouple was used to monitor the temperature of laser irradiated NR and solvent control samples. Since water does not absorb strongly at 792 nm, the temperature rise of the control solution is attributable to the thermocouple directly absorbing the laser. The bulk temperature rise due to the NRs was calculated by subtracting the temperature measured in the control solution from the NR solution.

RESULTS AND DISCUSSION

Characterization of NRs

The NRs synthesized by the non-seeding method were approximately cylindrical with hemispherical caps and monodisperse (Figure 1a). NRs were 34.9 ± 7.4 nm long by 10.3 ± 2.6 nm in diameter, with a mean AR = 3.6 ± 0.7 (Figure 1b). The NR longitudinal SPR (Figure 1c, solid line) coincided with the 792 nm spectral output of the fs pulsed laser (dashed line). The number of R_{18} molecules bound to NRs varied between 100 – 400 R_{18} per NR (Supporting Information).

Pulsed laser irradiation accelerates R_{18} release

We excited R_{18} loaded NRs with pulsed laser irradiation and quantified the amount of R_{18} released per NR ($R_{18,released}$) from the change in fluorescence intensity (ΔI) of the supernatant after NR separation by centrifugation,

$$R_{18,released} = \frac{(\Delta I)_{\lambda=EmissionPeak}}{f[NR]} \quad (1)$$

where f = 1.39 x 10^{12} $cps_{\lambda=583\ nm}$ / M in 10 mM CTAB is the fluorescence intensity per M of R_{18} for the fluorometer parameters detailed above, and $\Delta I = I_{exposed} - I_{unexposed}$ where $I_{exposed}$ and $I_{unexposed}$ are the fluorescence intensities (cps) of the supernatant of the irradiated and unexposed aliquots of the sample respectively. After 20 min of irradiation at a fluence of 110 μJ/cm^2, ΔI was positive (Figure 2a, purple line), indicating release of R_{18}. The ΔI was higher after irradiation with 220 μJ/cm^2 (blue line).

However, under higher laser fluences of 330, 440, and 550 μJ/cm^2 (green, orange, and red lines, respectively), the ΔI decreased. A shift of the peak fluorescence from 583 nm to 575 nm accompanied the increase in laser fluence.

We calculated the R_{18} release rate from the initial slope of the $R_{18,\ released}$ vs laser irradiation time (Figure 2b). At 110 μJ/cm^2 (Figure 2b, purple diamonds) the release rate was low, 0.006 ± 0.009 R_{18}/(NR·s). It increased to 0.028 ± 0.019 R_{18}/(NR·s) at 220 μJ/cm^2 (blue triangles). However, at 330 μJ/cm^2, (green triangles) the release rate was slightly lower, 0.025 ± 0.016 R_{18}/(NR·s). Increasing the fluence beyond 330 μJ/cm^2 (440 μJ/cm^2 and 550 μJ/cm^2, orange circles and red squares, respectively) resulted in an insignificant amount of apparent release.

These results indicate that the fs-pulsed laser irradiation of R_{18} loaded NRs accelerates the apparent release rate of R_{18}. The apparent release rate increases with laser fluence until 220 μJ/cm^2, after which it begins to decrease. We hypothesize that at fluences > 220 μJ/cm^2, the apparent release rate decrease is due to thermal degradation of the R_{18} while the actual release rate is probably increasing. Thus, we refer to the observable release rate as the apparent release rate. Further evidence of degradation is in the fluorescence intensity peak shift (Figure 2a) of the R_{18} at the high laser fluences.

The spread in the apparent release rate data represents the standard error weighted by the standard deviations of each individual data point. Thus, despite the wide error bars shown in Figure 2b, we have greater than 85% statistical confidence (Student's t-test) in the increased apparent release rate between 110 and 220 μJ/cm^2. However, since the apparent release rate values are very sensitive to the released molecule (R_{18}) and all the experimental and laser parameters, we suggest the general trend is more important than the actual values. This trend is apparent in data in Figure 2b, and it is reflected in the raw fluorescence data taken across all similar experiments (see Supporting Information).

With all the parameters as specified above, the optimal apparent release rate is 0.028 (R_{18}/(NR·s)). Given a 1 kHz laser repetition rate, the probability of releasing an R_{18} from a NR with any given pulse is 2.8×10^{-5}. This suggests that the apparent release rate can be doubled by doubling the repetition rate of

the laser to 2 kHz while keeping all the other parameters constant.

Controls on the release of R_{18}

We tested if the bulk temperature rise of the solution upon laser irradiation was responsible for the apparent R_{18} release rates. We measured the temperature rise of a 1 nM NR solution when irradiated at 330 $\mu J/cm^2$ to be ΔT = ~0.7 °C (Figure 3a). To determine if this temperature rise can explain the observed R_{18} release, we heated an aliquot of an R_{18} loaded NR sample to 30 °C (ΔT = 7 °C) in a water bath and quantified the R_{18} release. The fluorescence intensity of the heated aliquot (dots, Figure 3b) was the same as the unheated aliquot (line). This suggests that the increased apparent release rate is due to spatially confined temperature effects at the NR specific to ultrafast laser irradiation, not direct solvent heating by the laser.

We also explored whether laser irradiation of the R_{18} can explain the apparent R_{18} release rates. Irradiation of R_{18} associated with CTAB micelles with a fluence of 550 $\mu J/cm^2$ did not change the fluorescence intensity (Supporting Information). This suggests that the changes in R_{18} fluorescence intensity observed during R_{18} release are specific to excitation of the NR.

Finally, we explored whether the apparent R_{18} release rate is dependent on the aspect ratio of the NRs. Laser irradiation did not accelerate the apparent release rate of R_{18} from smaller aspect ratio NRs, whose longitudinal SPR absorption peak of 639 nm does not overlap the laser excitation (Supporting Information). This suggests that the increased apparent release rate is specific to NRs that have their longitudinal SPR tuned to the spectral output of the laser.

Exchange Mechanism

Because CTAB is amphiphilic and fluxional, it forms a bilayer at the NR-solvent interface.[10] CTAB exchanges from the bilayer on the NR surface to the solution, where it exists as isolated molecules or forms micelles. Because R_{18} is also amphiphilic, it exchanges from the CTAB bilayer on the NR surface to the solution, where a CTAB micelle stabilizes it (Scheme 1). Similar exchange mechanisms have been observed for other hydrophobic dyes interspersed in sodium dodecyl sulfate (SDS) and Triton X-

100 micelles.[32] Because R_{18} is minimally soluble in water, it has a strong tendency to intercalate into a CTAB micelle. Fluorescence spectroscopy showed that R_{18} was not fluorescent at low concentration of CTAB (Figure 4) and that the fluorescence intensity of R_{18} had a clear transition at CTAB's critical micelle concentration (cmc), ~1.2 mM,[33,34] suggesting that free, isolated R_{18} in solution is minimal. This exchange of R_{18} at the NR-solvent interface can be described by

(2)

where M_{Site} and NR_{Site} are an unoccupied R_{18} binding sites on CTAB micelles and NRs respectively, and the rate of release is

$$\frac{\mathrm{d}[R_{18,Micelle}]}{dt} = k_{off}[R_{18,Bound}][M_{Site}] - k_{on}[NR_{Site}][R_{18,Micelle}] \quad (3)$$

where $[R_{18,Micelle}]$ is the concentration of R_{18} solvated by CTAB micelles, $[R_{18,Bound}]$ is the concentration of R_{18} loaded into the CTAB bilayer on NRs. The concentration of unoccupied R_{18} binding sites in micelles is

$$[M_{Site}] = n_{CTAB}[M] - [R_{18,Micelle}], \quad (4)$$

the concentration of unoccupied R_{18} binding sites on NRs is

$$[NR_{Site}] = n_{NR}[NR] - [R_{18,Bound}], \quad (5)$$

n_{NR} and n_{CTAB} are the valency numbers of NRs and CTAB micelles respectively, $[NR]$ is the concentration Au NRs. $[M]$ is the concentration of CTAB micelles, and is defined as:

$$[M] = \left(\frac{[CTAB] - cmc}{n}\right) \quad (6)$$

where n is CTAB's aggregation number and $[CTAB]$ is the concentration of CTAB.

CTAB influences the binding and release of R_{18}

The details of the exchange mechanism have important consequences. Given that the cmc ~1.2 mM and n ~20,[33,34] at 1 nM NR and above the cmc ($[CTAB]$ ~ 10 mM), the concentration of CTAB micelles is much greater than the concentration of NRs ($[M] >> [NR]$). Thus, R_{18} tends to go into free micelles

because the positive term in eq 3 dominates. However, just below the cmc, [*M*] approaches zero, and R_{18} tends to bind to the NRs because the negative term in eq 3 dominates. Thus, according to eq 3, the CTAB concentration influences the rate at which R_{18} exchanges on and off the NR, particularly for [*CTAB*] ~ cmc.

We exploited the dependence of the release rate on [*CTAB*] during the process of loading R_{18} onto NRs and its release. Since maintaining [*CTAB*] < cmc favors R_{18} binding to the NRs, a low [*CTAB*] helps to load R_{18} onto NRs and maintain a low rate of R_{18} release once loading is complete, with negligible R_{18} loss over a period of days. However, if the [*CTAB*] is too low, the NRs are not stable and will aggregate. Additionally, since maintaining [*CTAB*] > cmc favors R_{18} release off the NRs, immediately prior to release experiments [*CTAB*] is increased to accelerate the rate of exchange to a measurable value.

Bulk heating accelerates R_{18} release and binding

We heated R_{18} loaded NRs in a water bath, and we measured the rate at which R_{18} both bound to and came off the NR. Released R_{18} ($[R_{18,Micelle}]$) increased with time (Figure 5a), and the rate of release ($d[R_{18,Micelle}]/dt$) increased with increasing temperature (Table 1). By fitting the rate of release at various temperatures to the Arrhenius equation (Figure 5a, inset), we obtained the activation energy of release, E_a *(off)*= 25.2 kcal/mol. R_{18}-NR association showed similar results (Figure 5b, Table 1), with a binding activation of E_a *(on)* = 26.1 kcal/mol. These E_a values are comparable to those observed for the exchange of pyrene-containing triglycerides in Triton X-100 micelles, E_a = 38.2 kcal/mol.[32]

We compared the rate of release of water bath heated and laser-irradiated samples. We found that the maximum apparent release rate (0.032 R_{18}/(NR·s) for 220 μJ/cm^2 laser fluence) for specific, local heating using fs pulsed laser irradiation before the effects of NR melting dominated corresponded to bulk sample heating using a water bath temperature between 40 and 50 °C.

Pulsed laser irradiation accelerates R_{18} binding

That the binding rate increases with water bath temperature suggests that laser irradiation can

accelerate not only the rate of release but also the reverse reaction, binding to the NRs. We introduced 1 nM NRs to 150 nM R_{18} in the presence of 1 mM CTAB and irradiated it with fluences of 220 and 330 μJ/cm^2 (Figure 6, blue filled triangles and green circles, respectively). [$R_{18,Micelle}$] decreased as a function of time due to binding to the NR, with a rate d[$R_{18,Micelle}$]/dt = -0.069 and -0.094 R_{18}/(NR·s), respectively (Table 1). However, higher fluence (440 μJ/cm^2, orange squares) did not increase the rate further. This behavior is similar to other laser irradiated samples at high fluence (Figure 2) and can be attributed to R_{18} thermal degradation.

Excess CTAB inhibits laser induced R_{18} binding

[*CTAB*] plays a key role in optimizing release and binding. Eqs 3 and 6 suggest high [*CTAB*] can inhibit R_{18} binding (-d[$R_{18,Micelle}$]/dt). To test this, we irradiated 1 nM NRs and 150 nM R_{18} in the presence of 10 mM CTAB. At 220 μJ/cm^2 the rate of R_{18} binding to the NR was 0.002 R_{18}/(NR·s) (Figure 6, blue dashed line and empty triangles), ~35× slower than when [*CTAB*] = 1 mM (Figure 6, blue solid line and filled triangles). These results, in combination with the fact that [*CTAB*] strongly influences the NR thermal interface conductance,[25] demonstrate that maintaining an appropriate [*CTAB*] is critical for controlling release.

NR melting correlates to the upper limits of laser accelerated release

Ultrafast-pulsed laser irradiation can melt Au NRs. Because the longitudinal SPR is a strong function of NR AR,[11] it can be used to monitor the onset of melting as a function of laser fluence[3,35,36] (Figure 7). The SPR peak position (inset) shifted under laser fluence as low as 220 μJ/cm^2, indicating the onset of melting. This coincides with the transition between an accelerated and decelerated exchange rate, suggesting that the observed decelerated exchange rate is primarily due to thermal degradation. Therefore, the fluence of 220 μJ/cm^2 maximizes the apparent release rate while minimizing R_{18} and NR destruction.

CONCLUSION

Ultrafast-pulsed laser irradiation accelerates the release of R_{18} from a NR surface. The effect is specific to NRs excited at their longitudinal SPR absorption band. Laser induced bulk solvent heating is not sufficient to accelerate release, so the release is due to local heating of the NR. However, thermal degradation of the R_{18} and the Au NRs limit the laser fluence increases that can effectively accelerate controlled release. A simple model explains the relationship between the kinetics of R_{18} release and the concentration of CTAB. While the mechanism presented is a simplified model of what occurs upon laser excitation of the NRs, it shows that by judicious choice of free ligand concentration and laser fluence, either release or capture of the target molecules by NRs can be achieved with laser irradiation. These results emphasize the importance of ligand surface chemistry and laser fluence on release rates. They have important implications for using ultrafast laser irradiation of NRs to deliver a broad range of molecules. Because laser-induced release from NRs is complex and involves multiple processes, future studies will examine how these processes independently influence release and binding rates.

ACKNOWLEDGMENT The authors thank Professor Andrei Tokmakoff, Kevin Jones and Lauren DeFlores for scientific discussions and use of their laser. We thank Victor Lelyveld for advice. We thank the Van Vliet Lab for use of their UV-Vis spectrophotometer, and MIT's Center for Materials Science and Engineering for use of their TEM.

Supporting Information Available. The details of R_{18} loading on Au NRs and the control experiments are available. The material is available free of charge via the internet at http://pubs.acs.org.

FIGURE CAPTIONS

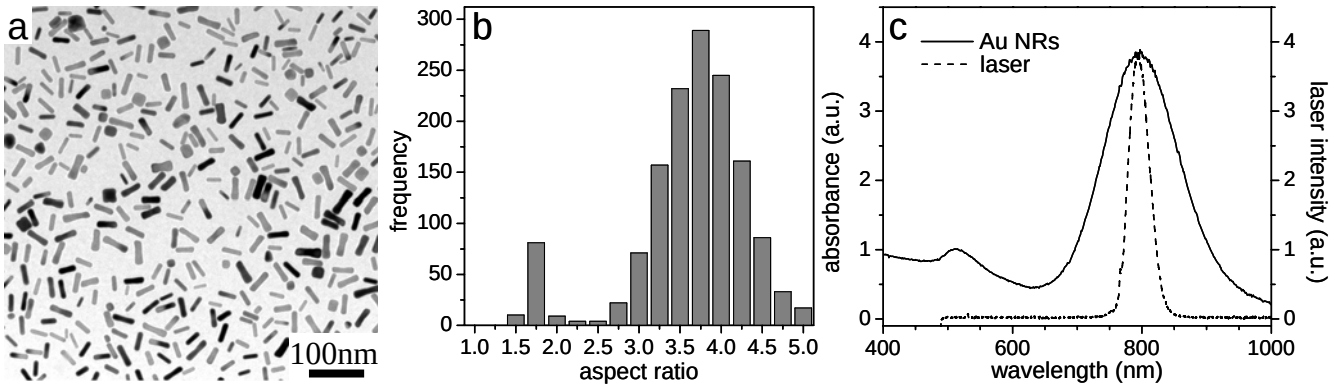

Figure 1. Characterization of Au NRs. a) TEM image of the Au NRs. b) Histogram of Au NR aspect ratio, <AR> = 3.6. The yield = number of NRs / total number of particles = 93%, where particles include rods and spheres. c) Optical absorption spectrum of Au NRs (solid black line) and spectral output of the laser excitation (black dashed line).

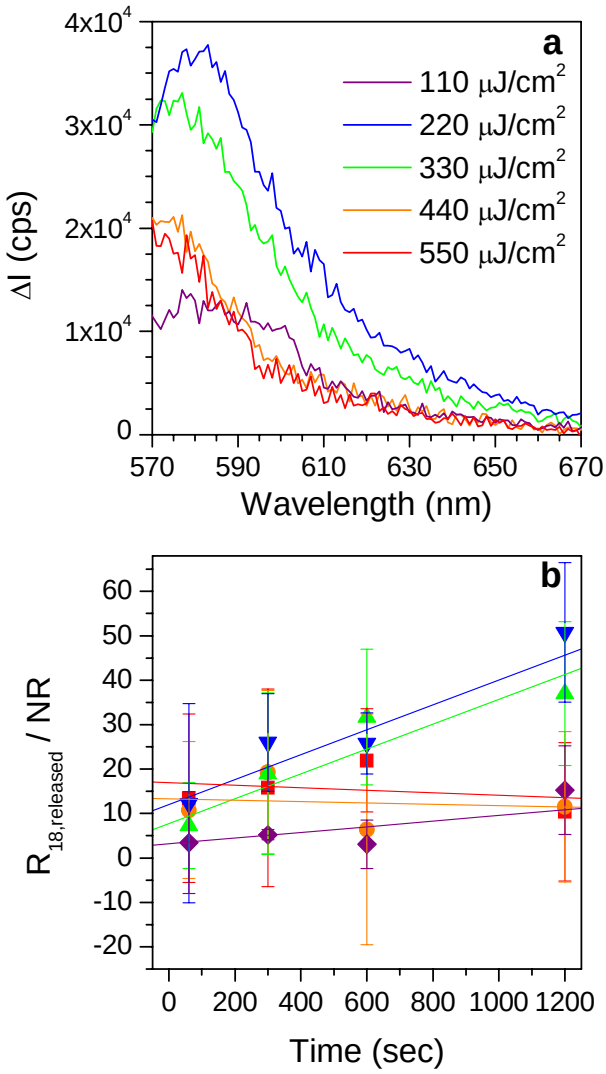

Figure 2. Release of R_{18} from NRs under laser irradiation. In both plots, the colors for laser fluences are: 110 μJ/cm^2 (purple), 220 μJ/cm^2 (blue), 330 μJ/cm^2 (green), 440 μJ/cm^2 (orange), 550 μJ/cm^2 (red). a) The difference between the supernatant fluorescence intensity of the laser irradiated and unexposed samples after NRs were separated from released R_{18} by centrifugation. Data for 20 min of laser exposure are shown. b) R_{18} per NR released as a function of laser irradiation time. Laser fluence: 110 μJ/cm^2 (purple diamonds), 220 μJ/cm^2 (blue down triangles), 330 μJ/cm^2 (green up triangles), 440 μJ/cm^2 (orange circles), 550 μJ/cm^2 (red squares). Error bars are the standard deviation of 3 repeats of data and lines are the least squares regression fit.

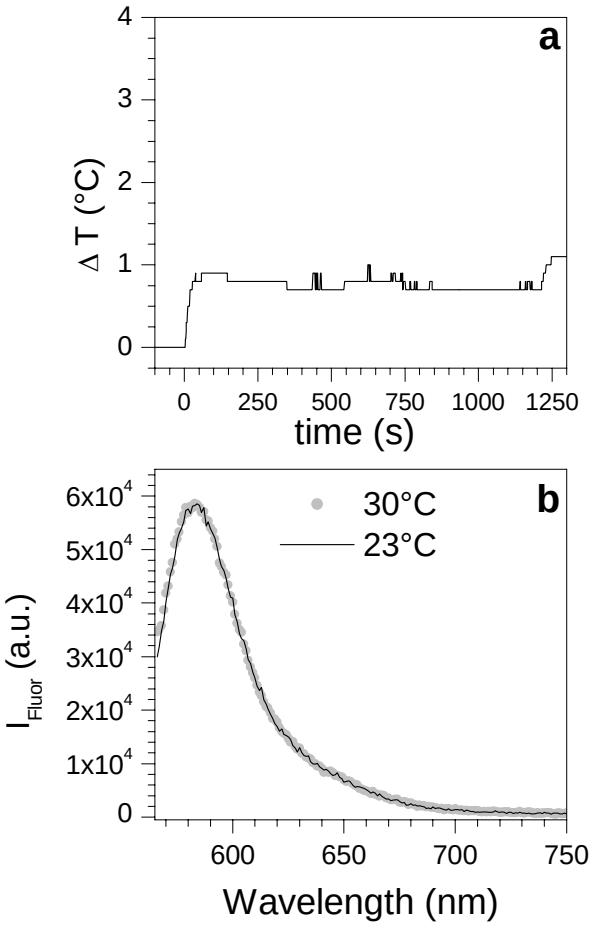

Figure 3. Control for bulk heating due to the laser. a) The bulk temperature rise of the sample due to NR heating. Pulsed laser irradiation began at time = 0 and continued for the duration of the test. The fluence was 330 μJ/cm^2, the wavelength was 792 nm, and the repetition rate was 1 kHz. b) Fluorescence intensity of the supernatants of an aliquot of sample heated to 30 °C (ΔT = 7 °C, points) in a water bath and an aliquot left at room temperature, 23° C, (line) for 20 min.

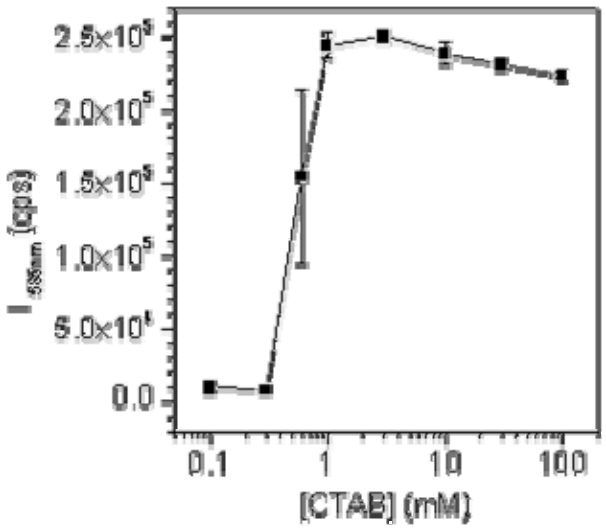

Figure 4. Fluorescence intensity of 100 nM R_{18} as a function of CTAB concentration. Error bars are the standard deviations of 3 sets of data.

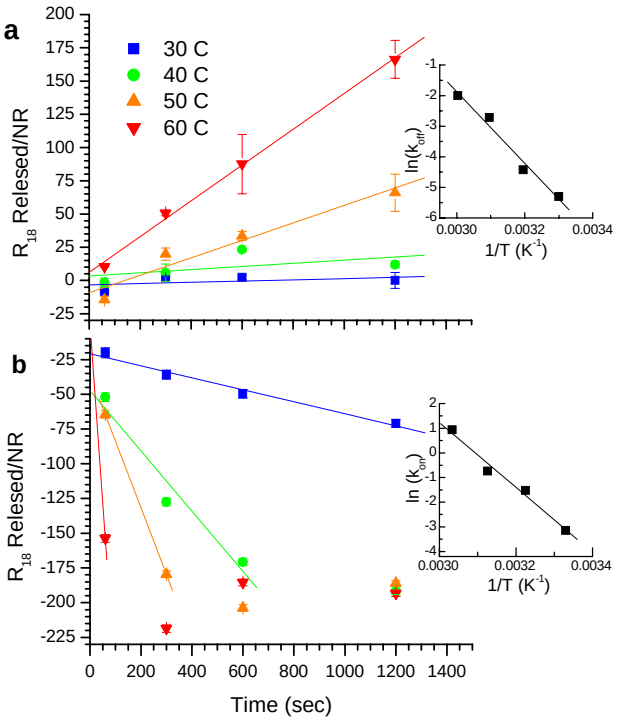

Figure 5. Induced release and binding of R_{18} when heated in a water bath. In both plots, water bath temperatures: 30 °C (blue squares), 40 °C (green circles), 50 °C (orange up triangles), 60 °C (red down triangles). Insets: Arrhenius plots. a) Release of R_{18} as a function of time. Error bars are the standard deviation of 2 repeats of data. b) Release of R_{18} as a function of time (negative numbers indicate binding). Samples are 1 nM NR, 1 mM CTAB and 150 nM R_{18}. Lines are the least squares regression fit for the initial, linear portions of these data.

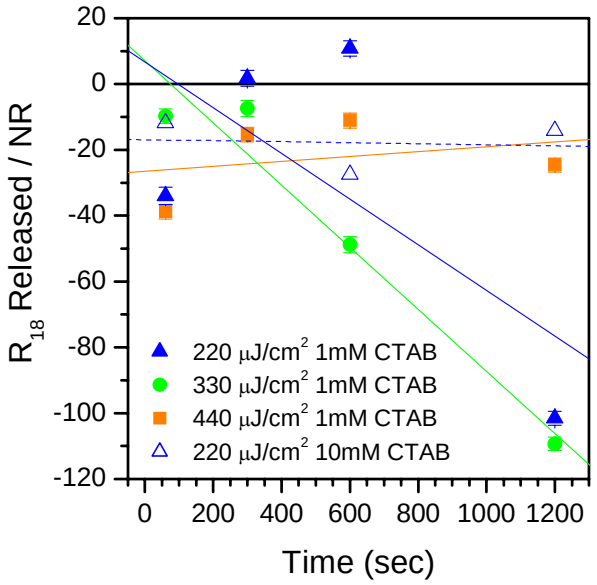

Figure 6. Binding of R_{18} to NRs under laser irradiation. Cumulative release (negative numbers indicate binding) of R_{18}. Filled data points are 1 nM NR, 1 mM CTAB and 150 nM R_{18}. Open data points are 1 nM NR, 10 mM CTAB and 150 nM R_{18}. Laser fluence: 220 μJ/cm^2 (blue triangles), 330 μJ/cm^2 (green circles) and 440 μJ/cm^2 (orange squares). Lines are the least squares regression fit and the binding rate is the initial slope of these data (Table 1).

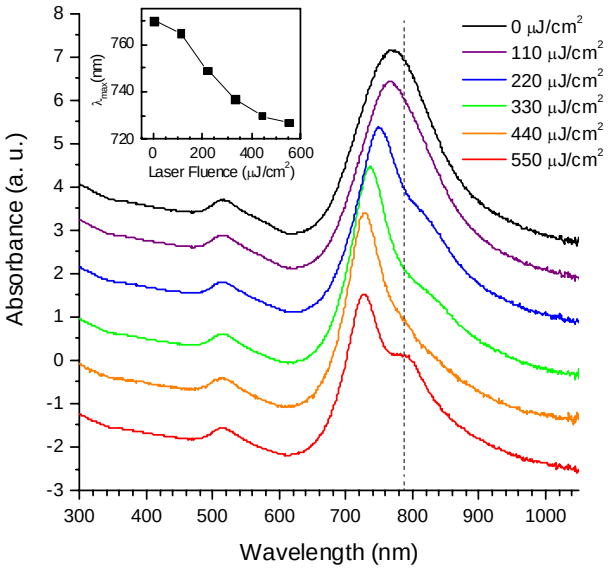

Figure 7. Optical absorption of NRs after 20 min of fs pulsed laser exposure. All data were normalized at λ = 375 nm. Dotted vertical line corresponds to the max laser output, and the spectra are offset for clarity. Laser fluence: 0 $\mu J/cm^2$ (black line), 110 $\mu J/cm^2$ (purple), 220 $\mu J/cm^2$ (blue), 330 $\mu J/cm^2$ (green), 440 $\mu J/cm^2$ (orange), 550 $\mu J/cm^2$ (red). Inset: longitudinal SPR wavelength (λ_{max}) as a function of laser fluence.

SCHEME TITLES

Scheme 1. R_{18} and Au NR - CTAB ligand exchange reaction.

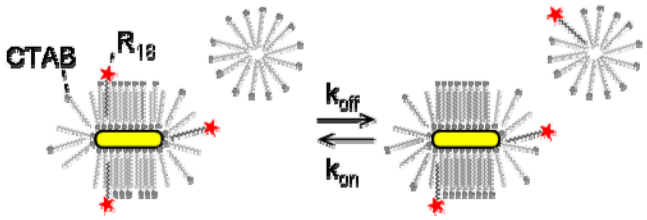

TABLES.

Table 1. R_{18} release and binding rates due to laser irradiation and water bath heating

release			binding		
water bath T (°C)	release rate (R_{18}/(NR·s))		water bath T (°C)	binding rate (R_{18}/(NR·s))	
30	0.004 ± 0.007		30	-0.042 ± 0.004	
40	0.012 ± 0.012		40	-0.217 ± 0.048	
50	0.066 ± 0.012		50	-0.479 ± 0.091	
60	0.135 ± 0.005		60	-2.56	
laser fluence (μJ /cm^2)	apparent release rate (R_{18}/(NR·s))	probability of release (R_{18}/(NR·pulse))	laser fluence (μJ/ cm^2)	apparent binding rate (R_{18}/(NR·s))	probability of binding (R_{18}/(NR·pulse))
110	0.006 ± 0.009	0.6×10^{-5}	110	N/A	N/A
220	0.028 ± 0.019	2.8×10^{-5}	220	-0.069 ± 0.054	6.9×10^{-5}
330	0.025 ± 0.016	2.5×10^{-5}	330	-0.094 ± 0.015	9.4×10^{-5}
440	-0.002 ± 0.007	N/A	440	0.007 ± 0.017	N/A
550	-0.003 ± 0.007	N/A	550	N/A	N/A

REFERENCES.

(1) Horiguchi, Y.; Niidome, T.; Yamada, S.; Nakashima, N.; Niidome, Y. *Chem. Lett.* **2007**, *36*, 952.

(2) Kitagawa, R.; Honda, K.; Kawazumi, H.; Niidome, Y.; Nakashima, N.; Yamada, S. *Jpn. J. Appl. Phys.* **2008**, *47*, 1374.

(3) Chen, C.-C.; Lin, Y.-P.; Wang, C.-W.; Tzeng, H.-C.; Wu, C.-H.; Chen, Y.-C.; Chen, C.-P.; Chen, L.-C.; Wu, Y.-C. *J. Am. Chem. Soc.* **2006**, *128*, 3709.

(4) Jain, P. K.; Qian, W.; El-Sayed, M. A. *J. Am. Chem. Soc.* **2006**, *128*, 2426.

(5) Takahashi, H.; Niidome, Y.; Yamada, S. *Chem. Commun.* **2005**, 2247.

(6) Qian, X. M.; Nie, S. M. *Chem. Soc. Rev.* **2008**, *37*, 912.

(7) Nikoobakht, B.; Wang, J.; El-Sayed, M. A. *Chem. Phys. Lett.* **2002**, *366*, 17.

(8) Hirsch, L. R.; Stafford, R. J.; Bankson, J. A.; Sershen, S. R.; Rivera, B.; Price, R. E.; Hazle, J. D.; Halas, N. J.; West, J. L. *Proc. Nat. Acad. Sci.* **2003**, *100*, 13549.

(9) Angelatos, A. S.; Radt, B.; Caruso, F. *J. Phys. Chem. B* **2005**, *109*, 3071.

(10) Murphy, C. J.; Sau, T. K.; Gole, A.; Orendorff, C. J. *MRS Bull.* **2005**, *30*, 349.

(11) Link, S.; El-Sayed, M. A. *Int. Rev. Phys. Chem.* **2000**, *19*, 409.

(12) Mie, G. *Ann. Phys.* **1908**, *330*, 377.

(13) Gans, R. *Ann. Phys.* **1912**, *342*, 881.

(14) Weissleder, R. *Nat. Biotechnol.* **2001**, *19*, 316.

(15) Ge, Z.; Cahill, D. G.; Braun, P. V. *J. Phys. Chem. B* **2004**, *108*, 18870.

(16) Anderson, R. R.; Parrish, J. A. *Science* **1983**, *220*, 524.

(17) Huang, X.; El-Sayed, I. H.; Qian, W.; El-Sayed, M. A. *J. Am. Chem. Soc.* **2006**, *128*, 2115.

(18) Norman, R. S.; Stone, J. W.; Gole, A.; Murphy, C. J.; Sabo-Attwood, T. L. *Nano Lett.* **2008**, *8*, 302.

(19) Pissuwan, D.; Valenzuela, S. M.; Miller, C. M.; Cortie, M. B. *Nano Lett.* **2007**, *7*, 3808.

(20) Aubin-Tam, M.-E.; Hamad-Schifferli, K. *Langmuir* **2005**, *21*, 12080.

(21) Petrova, H.; Juste, J. P.; Pastoriza-Santos, I.; Hartland, G. V.; Liz-Marzan, L. M.; Mulvaney, P. *Phys. Chem. Chem. Phys.* **2006**, *8*, 814.

(22) Perner, M.; Gresillon, S.; März, J.; von Plessen, G.; Feldmann, J.; Porstendorfer, J.; Berg, K. J.; Berg, G. *Phys. Rev. Lett.* **2000**, *85*, 792.

(23) Link, S.; El-Sayed, M. A. *J. Phys. Chem. B* **1999**, *103*, 4212.

(24) Murphy, C. J.; Sau, T. K.; Gole, A. M.; Orendorff, C. J.; Gao, J.; Gou, L.; Hunyadi, S. E.; Li, T. *J. Phys. Chem. B* **2005**, *109*, 13857.

(25) Schmidt, A. J.; Alper, J. D.; Chiesa, M.; Chen, G.; Das, S. K.; Hamad-Schifferli, K. *J. Phys. Chem. C* **2008**.

(26) Jana, N. R. *Small* **2005**, *1*, 875.

(27) Rasband, W. S. ImageJ; U. S. National Institutes of Health: Bethesda, MD, 1997-2008.

(28) Liao, H.; Hafner, J. H. *Chem. Mater.* **2005**, *17*, 4636.

(29) Alkilany, A. M.; Frey, R. L.; Ferry, J. L.; Murphy, C. J. *Langmuir* **2008**.

(30) Fernandez, M. S.; Fromherz, P. *J. Phys. Chem.* **1977**, *81*, 1755.

(31) Hoekstra, D.; Boer, T. d.; Klappe, K.; Wilschut, J. *Biochemistry* **1984**, *23*, 5675.

(32) Rharbi, Y.; Winnik, M. A. *Adv. Colloid Interface Sci.* **2001**, *89-90*, 25.

(33) Bahri, M. A.; Hoebeke, M.; Grammenos, A.; Delanaye, L.; Vandewalle, N.; Seret, A. *Colloid Surf. A* **2006**, *290*, 206.

(34) Tedeschi, A. M.; Franco, L.; Ruzzi, M.; Paduano, L.; Corvaja, C.; D'Errico, G. *Phys.*

Chem. Chem. Phys. **2003**, *5*, 4204.
(35) Horiguchi, Y.; Honda, K.; Kato, Y.; Nakashima, N.; Niidome, Y. *Langmuir* **2008**, *24*, 12026.
(36) Link, S.; El-Sayed, M. A. *J. Phys. Chem. B* **1999**, *103*, 8410.